



This is a repository copy of *Application of piece-wise linear system identification to solvent-based post-combustion carbon capture*.

White Rose Research Online URL for this paper:  
<http://eprints.whiterose.ac.uk/140071/>

Version: Accepted Version

---

**Article:**

Liao, P., Wu, X., Li, Y. et al. (4 more authors) (2018) Application of piece-wise linear system identification to solvent-based post-combustion carbon capture. *Fuel*, 234. pp. 526-537. ISSN 0016-2361

<https://doi.org/10.1016/j.fuel.2018.07.045>

---

Article available under the terms of the CC-BY-NC-ND licence  
(<https://creativecommons.org/licenses/by-nc-nd/4.0/>).

**Reuse**

This article is distributed under the terms of the Creative Commons Attribution-NonCommercial-NoDerivs (CC BY-NC-ND) licence. This licence only allows you to download this work and share it with others as long as you credit the authors, but you can't change the article in any way or use it commercially. More information and the full terms of the licence here: <https://creativecommons.org/licenses/>

**Takedown**

If you consider content in White Rose Research Online to be in breach of UK law, please notify us by emailing [eprints@whiterose.ac.uk](mailto:eprints@whiterose.ac.uk) including the URL of the record and the reason for the withdrawal request.



[eprints@whiterose.ac.uk](mailto:eprints@whiterose.ac.uk)  
<https://eprints.whiterose.ac.uk/>

# Application of piece-wise linear system identification to solvent-based post-combustion carbon capture

Peizhi Liao<sup>a</sup>, Xiao Wu<sup>a</sup>, Yiguo Li<sup>a,\*</sup>, Meihong Wang<sup>b,\*</sup>, Jiong Shen<sup>a</sup>, Adekola Lawal<sup>c</sup>, Chuanlong Xu<sup>a</sup>

<sup>a</sup>Key laboratory of Energy Thermal Conversion and Control of Ministry of Education, Southeast University, Nanjing 210096, China

<sup>b</sup>Department of Chemical and Biological Engineering, University of Sheffield, Sheffield S1 3JD, UK

<sup>c</sup>Process Systems Enterprise Ltd, 26-28 Hammersmith Grove, London W6 7HA, UK

---

## Abstract

Solvent-based post-combustion carbon capture (PCC) is currently the most promising method to reduce CO<sub>2</sub> emission. To achieve a plant-wide controller for flexible operation, it is necessary to develop a data-driven model to understand the dynamic characteristics of PCC plant. This paper aims to: (i) carry out system identification to develop a data-driven model and (ii) provide insights into the nonlinear dynamics among the key variables from the PCC process in a wide operating range. These key variables include: CO<sub>2</sub> capture rate, reboiler temperature, condenser temperature and lean solvent temperature. Pilot-scale PCC process implemented in gCCS was used to generate simulation data for system identification and model comparison. Linear single-input-single-output (SISO) transfer function models were firstly developed at different capture rates. Open loop step tests on identified models were then introduced to report the dynamics of key variables in various operating conditions and to indicate the level of system nonlinearity graphically. The nonlinearity analysis was carried out to investigate the system nonlinearity distribution in a quantitative manner. Based on the nonlinearity analysis, a multi-input-multi-output (MIMO) piece-wise model was proposed to simulate the nonlinear characteristics of PCC plant. The piece-wise model shows a satisfactory agreement with gCCS simulation data. Results of this study successfully demonstrate the nonlinear behavior of the solvent-based PCC process, which can be applied in the design of flexible plant-wide controllers.

Keywords: Post-combustion carbon capture; Solvent-based carbon capture; System identification; Piece-wise model; Nonlinearity analysis

---

## 1. Introduction

### 1.1 Background

Global warming has increasingly drawn public attention. Extensive research has been performed to combat this trend. The Intergovernmental Panel on Climate Change (IPCC) stated that CO<sub>2</sub> contributed to about 50% of the increasing temperature in the earth surface among all the greenhouse gas [1]. Most of the CO<sub>2</sub> emissions originate from combustion of fossil fuels in large-scale power plants. For the near future, it is necessary to take measures to reduce CO<sub>2</sub> emission from these sources since fossil fuel is still attractive to meet future energy demands due to its rich availability, large energy density and low cost [1].

Among all the approaches, solvent-based PCC technology is viewed as the most mature option for existing power plants [3]. It offers advantages over other capture technologies because of high selectivity and pure CO<sub>2</sub> stream collection [3]. It can also be retrofitted as an end-of-pipe solution.

In the past decades, research efforts have been devoted to understanding the intricate nature of this carbon capture process. Solvent regeneration is energy intensive and it requires a lot of steam extracted from power plants. Given its high energy requirement, the solvent regeneration process will reduce the overall power plant efficiency significantly [4]. It is therefore important to minimize the energy demand and make more steam available for power generation [5]. However, it is still a matter of concern to find a trade-off to balance CO<sub>2</sub> removal rate and energy cost under the time-varying economic conditions. In this regard, there is a need to develop a flexible plant-wide control structure in order to achieve optimal performance in the presence of disturbance, load-changing and other scenarios. The nonlinear dynamic characteristics of PCC process need to be analyzed to provide information for the advanced controller's design.

### 1.2 Motivation

To study the dynamics of solvent-based PCC plant, several first-principle models have been developed (Lawal et al [5, 6, 7]). These models have been proven to be able to closely predict the real process. A number of carbon capture pilot plants are now

45 available worldwide to provide steady-state or dynamic validation data (Dugas [8], Biliyok et al [9]). Nevertheless, it is clear that  
46 the simulation with first-principle models is computationally demanding. This makes controller design based on first-principle  
47 models difficult. Therefore, it is necessary to use a data-driven black-box identification method to serve as an alternative. On the  
48 other hand, most of the studies for PCC plant are focused on the linear models developed at a fixed operating point. Under varying  
49 operating conditions, the transient behavior of PCC plant will change and it would be difficult for linear models to simulate the  
50 nonlinear features. The linear model's failure to capture the nonlinear dynamics of the PCC plant will deteriorate the control  
51 performance. In order to develop a model predictive controller for wide-range capture rate change, Wu et al [10] proposed a simple  
52 nonlinear distribution analysis for solvent-based PCC plant. However, since multi-variable model is used in the analysis, the  
53 nonlinearity for a certain input-output loop cannot be revealed in detail. Motivated by these shortcomings, an investigation was  
54 carried out to further understand the operational features of a PCC plant over a wide range of operating conditions, and to identify  
55 possible control difficulties which may arise.

### 56 1.3 Aim of the study and main novel contributions

57 This study aims to identify a plant-wide black-box model based on piece-wise linear identification method. There are two major  
58 novelties in this paper:

- 59 • A fuzzy-based piece-wise model which can approximate the nonlinear dynamic features of a PCC process from 50% - 95%  
60 capture rate is achieved at a fixed power plant load. This model can be used for the plant-wide controller design.
- 61 • Detailed nonlinear characteristics of key variables in PCC process are researched quantitatively. These key variables include:  
62 CO<sub>2</sub> capture rate, reboiler temperature, condenser temperature and lean solvent temperature.

### 63 1.4 Outline

64 The paper is organized as follows: Section 2 presents the available literature review on modelling and identification of PCC  
65 process. Section 3 generates the simulation data of solvent-based PCC process in gCCS platform and uses these data to identify  
66 linear local SISO system models from 50% to 95% capture rate. In Section 4, a critical sensitivity analysis is performed by  
67 introducing step changes in the input variables. Nonlinearity degree analysis is carried out in Section 5. Section 6 presents the  
68 MIMO fuzzy-based piece-wise model. Conclusions are drawn in Section 7.

## 69 2. Literature review

70 Mass transfer and chemical reaction are two key factors to consider in modelling solvent-based PCC process. To describe the  
71 mass transfer process, two approaches are usually used in most studies: the equilibrium-based approach and the rate-based approach.  
72 In Lawal et al [6], a critical comparative evaluation showed that a rate-based model gives better agreement with experimental data.

73 To date, many studies on dynamic modelling have been implemented. In Kvanstal et al [11], a dynamic model of standalone  
74 absorber column in rate-based modelling approach was presented. This model was simulated in two load-varying cases, namely,  
75 start-up and load-reduction, to evaluate the operability of absorber. In Ziari et al [12], a standalone stripper model was built in  
76 Aspen Customer modelling environment. Dynamic simulation was carried out to run the stripper flexibly during the period of high  
77 electricity demand and price.

78 However, the limitation of the aforementioned publications is that stand-alone model cannot represent the whole PCC process  
79 due to the intricate nature with regard to high nonlinearity and process interactions. Therefore, a dynamic model considered  
80 interacted units is significant to combine them together as a whole plant. Lawal et al [5] presented a dynamic model including  
81 absorber, stripper and recycle. Based on a comparative assessment, the whole process model gives more accurate results in  
82 predicting temperature profile than standalone columns. In their follow-up work [7], a scaled-up integrated model to industrial size  
83 of a 500 MW coal-fired subcritical power plant was made available. This work gave a preliminary technical evaluation of integrated  
84 PCC process and power plant. Due to lack of experimental data, dynamic validation is very rare. Biliyok et al [9] presented data at  
85 transient scenarios for dynamic model validation. In the same paper, dynamic process analysis proved that mass transfer is the  
86 major factor which limits CO<sub>2</sub> absorption.

87 First-principle model provides the advantage to realize accurate simulation, as well as understanding the underlying dynamics

88 of the process. Nevertheless, as stated previously, first-principle model is computational intensive and it is hard to realize. Thus,  
89 carrying out black-box identification has emerged as an attractive alternative to first-principle dynamic modelling.

90 Arce et al [13] used Matlab<sup>TM</sup> identification toolbox (Ljung [14]) to obtain a linear model for solvent regeneration process. This  
91 model was composed of a first-order linear discrete transfer function with a sampling time of 200 ms. However, a first-order model  
92 cannot mimic the dynamic features compared with a higher order model. For capturing nonlinear characteristics, Manaf et al [15]  
93 employed a multivariable nonlinear autoregressive with exogenous input (NARX) model. To reduce computational demand,  
94 identified model for absorber, rich/lean heat exchanger and stripper were acquired separately and united as a 4-input-3-output PCC  
95 model. The distinguished contribution of [15] is that the rich/lean heat exchanger, a major investment and operating penalty unit  
96 [16], was considered in the modelling. However, this paper did not provide available control structure to operate heat exchanger.

97 Li et al [17] presented a bootstrap aggregated neural approach to build a multiple-inputs-single-output (MISO) dynamic model.  
98 Results showed its superiority in predicting capture level compared with conventional neural networks. One-step-ahead and multi-  
99 step-ahead prediction were used as the neural network input. It was found that one-step-ahead prediction is more accurate, because  
100 the prediction errors were accumulated every sampling time in a multi-step-head prediction and this would increase the prediction  
101 error at the following sampling time.

102 In data-driven modelling of a nonlinear system, the most typical way is to use polynomial functions to approximate the  
103 nonlinearity [18]. But the model order resulted from the polynomial function is always high, especially for a complicated industrial  
104 process. It is not always easy to solve these equations analytically. There is another option for nonlinear approximation which uses  
105 piece-wise-linear (PL) functions. PL functions aim to approximate the nonlinear features by a combination of linear pieces. In  
106 general, the nonlinear model produced by a serial of linear models is expected to result in an easier implementation, theoretical  
107 analysis and calculation [19]. The proposed work tries to use a piece-wise modelling method to simulate the real PCC process, and  
108 also to investigate the nonlinear features.

### 109 3. Process description and local model identification

#### 110 3.1. Process description

111 gCCS simulation software was developed based on gPROMS modelling platform to support simulation and design of power  
112 plants, carbon capture, transport and storage [20]. It was developed by Process Systems Enterprise (PSE) Ltd in London and it is  
113 commercially available. As shown in Fig. 1, a pilot-scale dynamic model of solvent-based PCC process is implemented in gCCS  
114 environment. Process model used in gCCS is based on the detailed dynamic model in Lawal et al [5]. The equipment parameters  
115 are kept the same at all the simulation scenarios. To validate the identified models in this manuscript, dynamic experimental data  
116 is not available in the current publications, the simulation data from gCCS was therefore used for model identification and  
117 comparison.

118 The working process of the considered solvent-based PCC plant is as follows: flue gas from a power plant or an industrial  
119 process is firstly cooled down to 40-50°C for a higher absorption performance, then it is fed into the bottom of absorber and comes  
120 in contact with lean MEA solvent counter-currently. CO<sub>2</sub> is absorbed chemically and the treated gas leaves from the top side of  
121 absorber. Rich (CO<sub>2</sub> concentration amine) solvent from the bottom of absorber is then pumped into the cross-heat exchanger and  
122 preheated by hot lean (CO<sub>2</sub> concentration amine) solvent before entering the stripper. Low-pressure steam from power plants is  
123 used in the reboiler. As a result of heat, the chemical bonds are thermally broken, releasing CO<sub>2</sub>. The operational temperature of  
124 the reboiler needs to be maintained within 383-393k to avoid amine degradation [21]. The vapor from the top of stripper is  
125 condensed and separated in the condenser, water and amine are then refluxed back to stripper. Finally, the lean amine solution from  
126 the reboiler is cooled in the cross-heat exchanger by exchanging heat with rich CO<sub>2</sub> concentration amine before returning to  
127 absorber. In general, a buffer tank containing a cooling coil is needed to keep water and MEA balance, as well as maintaining lean  
128 solvent temperature.

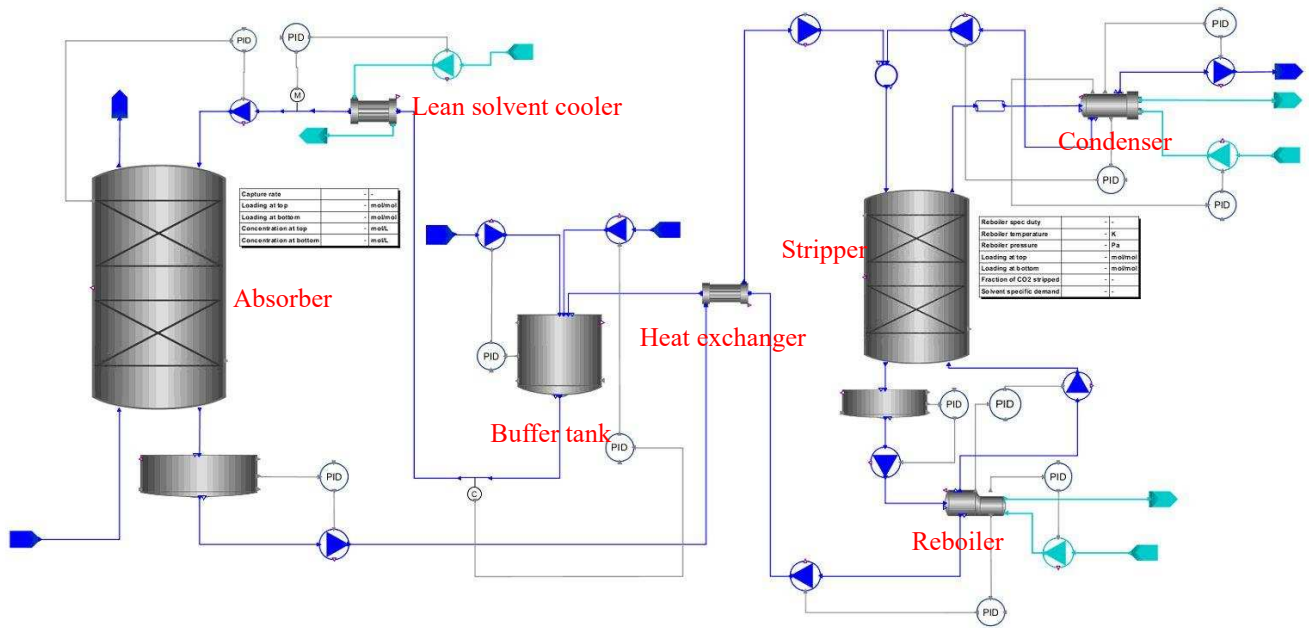


Fig 1. Model topology in gCCS

The next step in this section is to select the manipulated and controlled variables. Lean solvent flowrate and steam flowrate are the key variables influencing the characteristics of PCC plant. The control structures between lean solvent flowrate/steam flowrate and capture rate/reboiler temperature are mostly discussed in previous studies [22, 23]. Moreover, this study considers the effects of condenser temperature and lean solvent temperature since they are closely related to the operation of PCC plant. Condenser temperature is related to the purity of CO<sub>2</sub> product [24]. Therefore, for a higher concentration of CO<sub>2</sub> product, it is necessary to maintain low condenser temperature since this has the benefit of reducing compression costs. Aroonwilas and Tontiwachwuthikul [25] reported that an increase in lean solvent temperature (at the Absorber top inlet) from 298K to 309K can lead to the increase of CO<sub>2</sub> absorption ability. Beyond 309K, a further increase in the temperature to 318K may result in a reduction of overall mass transfer coefficients. Therefore, lean solvent temperature is a vital parameter to be controlled for the best absorption performance.

For this reason, this paper mainly studies the dynamic characteristics of these key variables. As listed in Table 1, the lean solvent flow rate to absorber ( $u_1$ ), steam flowrate to reboiler ( $u_2$ ), cooling water flowrate to condenser ( $u_3$ ) and cooling water flowrate to cooler ( $u_4$ ) are taken as 4 major manipulated variables, while capture rate ( $y_1$ ), reboiler temperature (lean solvent side) ( $y_2$ ), condenser temperature ( $y_3$ ) and lean solvent temperature ( $y_4$ ) are corresponding controlled variables.

Table 1. Steady-state controlled values

	Manipulated variables	Controlled variables	Setpoint
Control loop 1	Lean solvent flowrate	Capture rate	/
Control loop 2	Steam flowrate	Reboiler temperature	383 K
Control loop 3	Cooling water flowrate to condenser	Condenser temperature	313.15 K
Control loop 4	Cooling water flowrate to cooler	Lean solvent temperature	313 K

### 3.2. Steady-state values

This section carries out the steady-state analysis on these key variables. The steady-state values will provide preliminary information on the steady-state features of PCC plant.

In this paper, capture rate is used as scheduling variable and to determine operating condition of PCC plant. This is due to its inherent nature of indicating the fulfillment of carbon absorption requirement in terms of environmental protection. Under this control circumstance (in Table 1), capture rate is varied in large scale while reboiler temperature, condenser temperature and lean solvent temperature are remained constant. Therefore, capture rate can be used to reveal the variation of working conditions for PCC plant and it is an important variable to be considered.

158 Steady-state simulations are carried out by adjusting capture rate setpoint from 50% to 95% in intervals of 5%. All the  
 159 manipulated and controlled variables are collected in Table 2 and plotted in Fig. 2. From the figure, it can be observed that all the  
 160 manipulated variables show an upward trend with increasing capture rate. Lean solvent flowrate and steam flowrate are  
 161 approximately proportional to the capture rate, while cooling water flowrate to cooler experiences a sharp increase when capture  
 162 rate reaches 90%. The cooling water flowrate to the condenser increases gradually until it reaches 90% capture rate. Above 90%  
 163 capture rate, the flowrate starts to decline.

164 Table 2. Steady-state manipulated values

MVs	Lean solvent flow rate (kg/s)	Steam flowrate (kg/s)	Cooling water flowrate to condenser (kg/s)	Cooling water flowrate to cooler (kg/s)
50% capture rate	0.70801	0.0368226	0.162656	0.4388
55% capture rate	0.78350	0.0421757	0.166775	0.5239
60% capture rate	0.85924	0.0477303	0.170163	0.6234
65% capture rate	0.93545	0.0534870	0.172964	0.8099
70% capture rate	1.01332	0.0595083	0.175292	0.9964
75% capture rate	1.09216	0.0657443	0.177172	1.2504
80% capture rate	1.17361	0.0722941	0.178686	1.6191
85% capture rate	1.25718	0.0791476	0.179722	2.2229
90% capture rate	1.34627	0.0865317	0.180230	3.4151
95% capture rate	1.45123	0.0952342	0.179464	7.5704

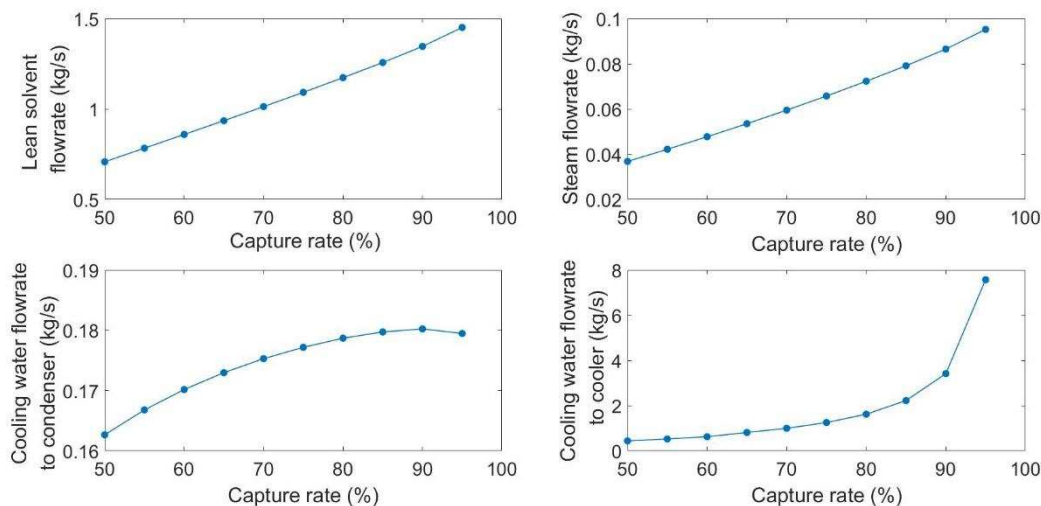


Fig. 2 Steady-state manipulated values

165 From Table 2 and Fig. 2, we can have a preliminary understanding on how these inputs will change at different capture rates. A  
 166 quantitative analysis of the process requires the identification of system models to provide dynamic parameter information, such  
 167 as time constant and settling time.

### 170 3.3. Local model identification

171 At different capture rates (50%, 60%, 70%, 80%, 90%, 95% capture rate), local models between manipulated variables and  
 172 controlled variables (As listed in Tables 1) are obtained using System Identification Toolbox in MATLAB [14]. SISO transfer  
 173 function is selected as the model type because it is simple in identification and convenience in model analysis.

174 Such an identification technique utilizes input-output data to estimate mathematical model. The information provided by the  
 175 input-output data will influence the accuracy of the identified model. Considering the large time constant of PCC process, low  
 176 frequency pseudo-random binary sequence (PRBS) signal with a sampling time of 5 secs is designed as input to persistently excite  
 177 the PCC system and provide enough information. An example of PRBS excitation data in lean solvent flowrate ( $u_1$ ) at 90% capture  
 178 rate is given in Fig. 3.

179  
180  
181  
182  
183

To generate data for identification, the PCC process is in open loop. The input perturbation is applied to each input channel individually. All the identification and comparison data are generated in the gCCS modelling software. Before performing identification, all the data are pre-treated to remove mean value, outliers and noise. Singular value decomposition (SVD) on the Hankel matrix constructed from input-output data is conducted to estimate the model order [26]. A total number of 16 transfer functions (4 inputs by 4 outputs) are identified at every capture rate. The details of the identified model are available in the Appendix.

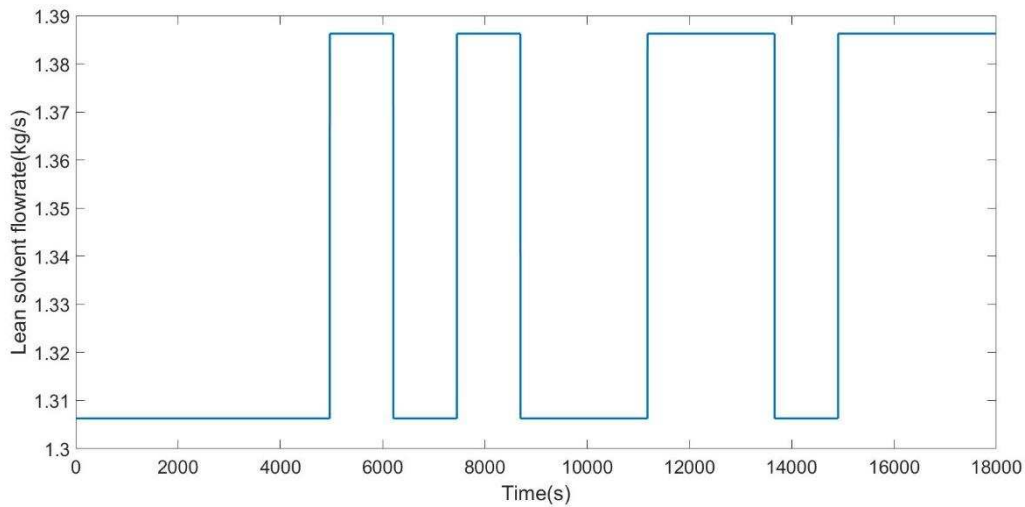


Fig.3. Excitation data of lean solvent flowrate at 90% capture rate

184  
185

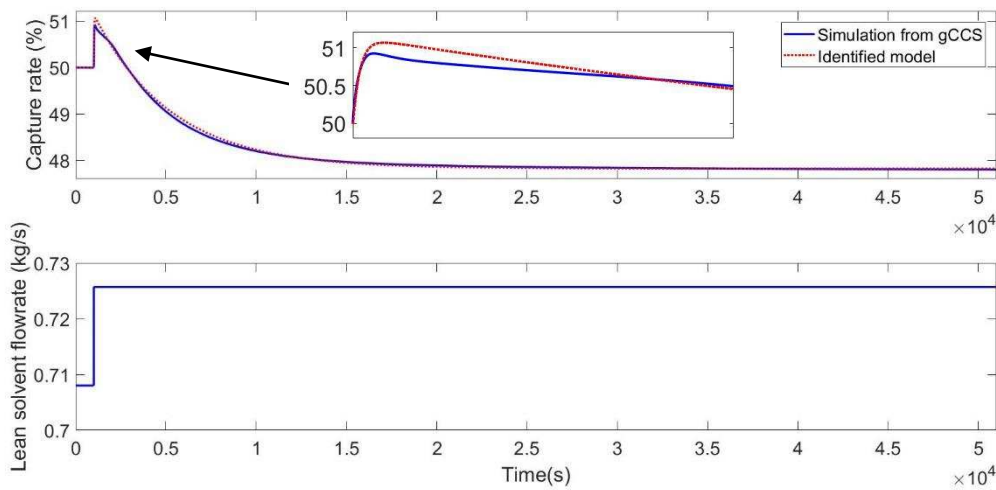


Fig. 4. Comparison of lean solvent flowrate – capture rate model at 50% capture rate

186  
187

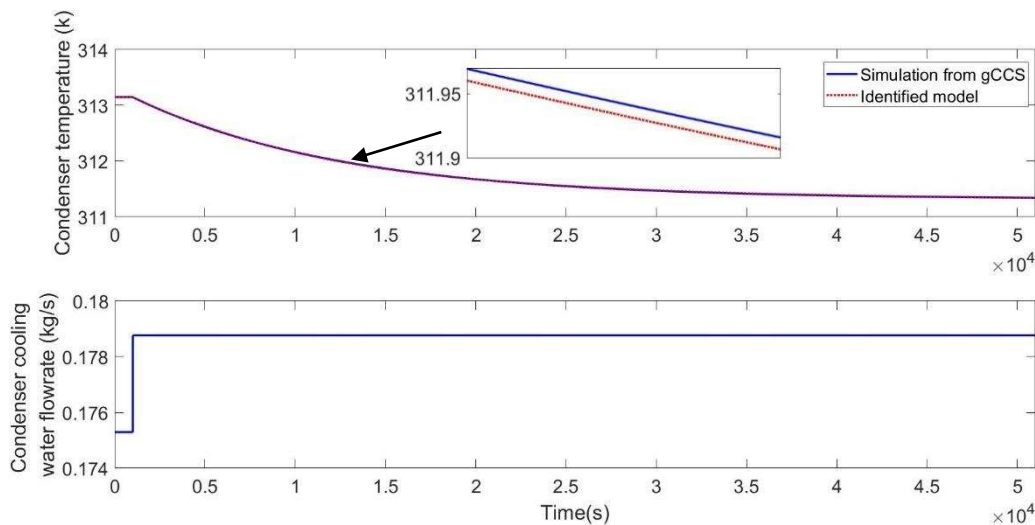


Fig. 5. Comparison of condenser cooling water flowrate – condenser temperature model at 70% capture rate

188  
189

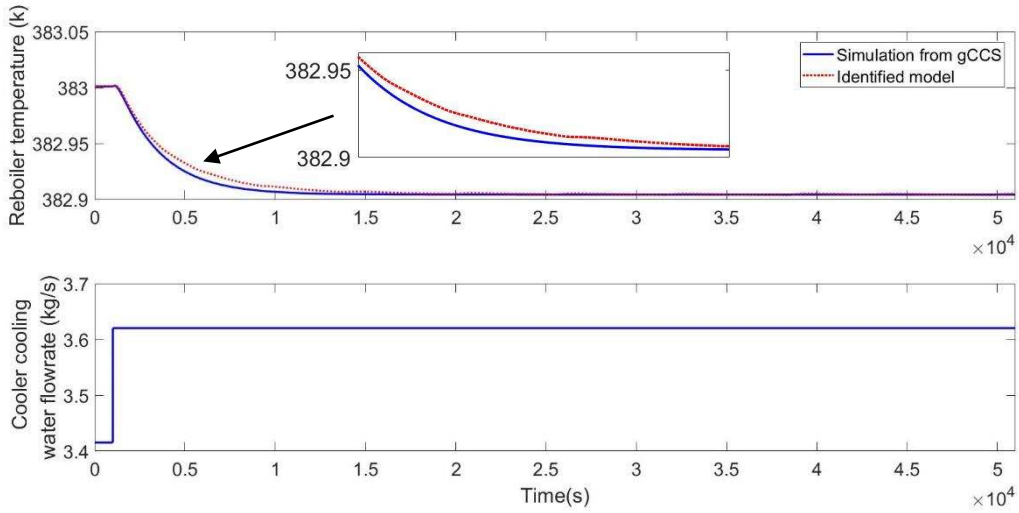


Fig. 6. Comparison of cooler cooling water flowrate – reboiler temperature model at 90% capture rate

Step response tests are introduced to compare the identified local models with simulation data. As shown in Figs. 4-6, the local models are in satisfactory agreement with the simulation data from gCCS software. However, due to the space limits, only 3 models at 50%, 70% and 90% capture rate are chosen as examples. All the remaining models also give good results when compared with corresponding simulation data.

#### 4. Open-loop step response analysis

Based on the identified local models in Section 3.3, open-loop step response tests are carried out under 50%, 60%, 70%, 80%, 90% and 95% capture rates for the major variables listed in Table 1. This study can provide the dynamic information of these variables, such as time constant and settling time. Besides, the step response test can inherently reveal how the input influences the corresponding output under varying operating conditions. This can enhance the understanding of nonlinear dynamic characteristics of PCC plant in a qualitative manner.

A relative variation of input  $\Delta u$  with a fixed value of 0.1 is performed in every scenario. The relative input  $\Delta u$  is expressed in Equation (1).

$$\Delta u = \frac{u - \bar{u}}{\bar{u}} \quad (1)$$

where  $u$  denotes the absolute value introduced to input channel while  $\bar{u}$  denotes the steady-state values in different capture rates. Likewise, the model output is treated in the same way. The relative variations of outputs are depicted in Figs. 7-10.

All the step response curves are presented in the same benchmark in order to make reasonable performance comparison. To run the simulation, only one input is varied and the others remain constant.

##### 4.1. Step changes in lean solvent flowrate

Using lean solvent flowrate to regulate capture rate is the most typical control option. It offers the advantage of faster response and lower overshoot [27]. To gain insight into the transient behaviors of this loop, a relative step change  $\Delta u$  with a positive amplitude of 0.1 is introduced to the lean solvent flowrate in the step time of 1000 secs. The relative output responses are displayed in Fig. 7. It can be observed that capture rate increases sharply at the start of simulation for all cases, revealing the instant influence of step change. Simultaneously, the solvent lean loading (mol CO<sub>2</sub> /mol MEA) also increases, leading to the decrease of capture rate after 1300 secs. Therefore, final value of the capture rate is lower than its initial value. This shows a typical non-minimum phase feature, which may lead to the fluctuation of manipulated variable and it may also deteriorate control performance. Therefore, an advanced control technique, e.g. pole assignment method, is advised to deal with this problem. Besides, the model time constants at different capture rates are almost the same. Steady-state gains decrease with the increase of capture rate up to 90%, while the gain in 95% capture rate has a sudden increase.



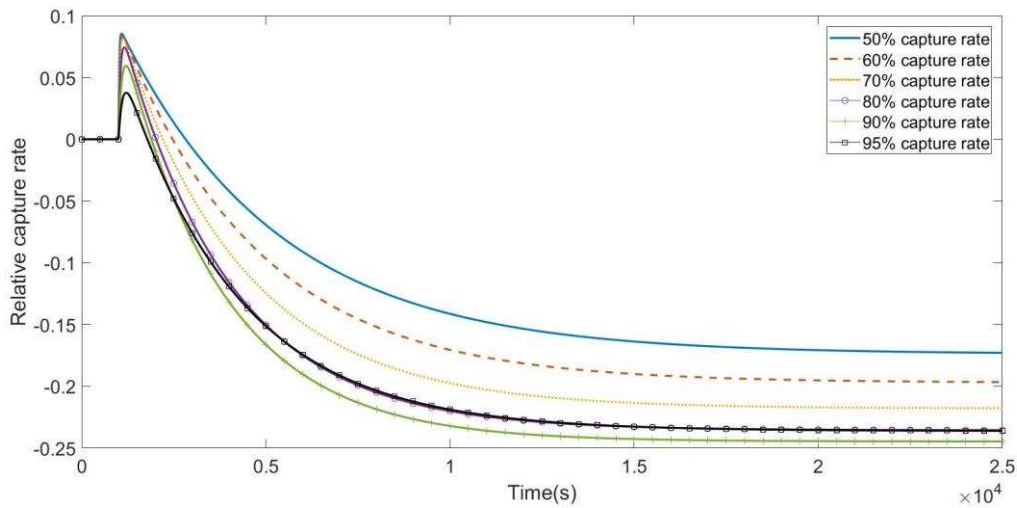


Fig. 7. Relative capture rate with the step change in lean solvent flowrate

#### 4.2. Step changes in reboiler steam flowrate

Reboiler temperature is an important parameter which plays a key role in MEA regeneration process. It is regarded as the indicator of lean loading [23], which in turn reflects water makeup and capture rate controls. In this section, investigation of the effect of a positive increase in reboiler heat duty is carried out. The required reboiler heat duty is supplied from the low-pressure steam turbine in power plant. A relative increase of 0.1 in the steam flowrate is implemented in a relatively short period of time. Consequently, there is a significant increase in reboiler temperature, as observed in Fig. 8. The perturbations' amplitude raises gradually with increasing capture rate. It appears a relatively smooth change in the output response.

#### 4.3. Step changes in cooling water flowrate to condenser

Condenser temperature is inversely related to the CO<sub>2</sub> purity [24]. Changing the flowrate of cooling water provides a potential option for the manipulation of the system. In this section, the open-loop performance of the condenser is investigated by increasing the flowrate of cooling water passing through the condenser. The process was simulated over a period of 50000 secs with a relative increase of 0.1 in the step time of 1000 secs. As shown in Fig. 9, condenser temperature reaches steady state after 40000 secs or 10 hrs, which indicates a very large inertia in the condenser. Furthermore, with decreasing capture rate, the settling time in condenser increases. Under this circumstance, condenser temperature will not be easily affected by other manipulated variables due to its large time constant.

#### 4.4. Step changes in cooling water flowrate to cooler

According to [25], lean solvent temperature will affect the overall mass transfer coefficients of absorber column. Therefore, lean solvent temperature needs to be controlled for the higher absorption performance. In this paper, we used a counter-current heat exchanger (As shown in Fig. 1) to maintain lean solvent temperature. This may reduce the system ability to resist disturbances in lean solvent flowrate, but the time necessary for controlling lean solvent temperature can be reduced, since it doesn't have massive liquid storage. Fig. 10 shows the output response in the presence of step change in the flowrate of cooling water entering the cooler. The amplitude of a relative step change in flowrate of cooling water is 0.1. It can be observed that the cooling water flowrate has an instant influence on the lean solvent temperature. This is due to the large heat transfer coefficient and heat transfer area in the cooler. After that, the lean solvent temperature decreases gradually, this is influenced by the decrease in reboiler temperature. On the other hand, the model in 50% capture rate has the highest steady state gains and longest settling time. With the increase of capture rate, these two parameters decrease dramatically. Preliminary results can be obtained to indicate a much stronger nonlinearity in the cooler compared with other mentioned units.

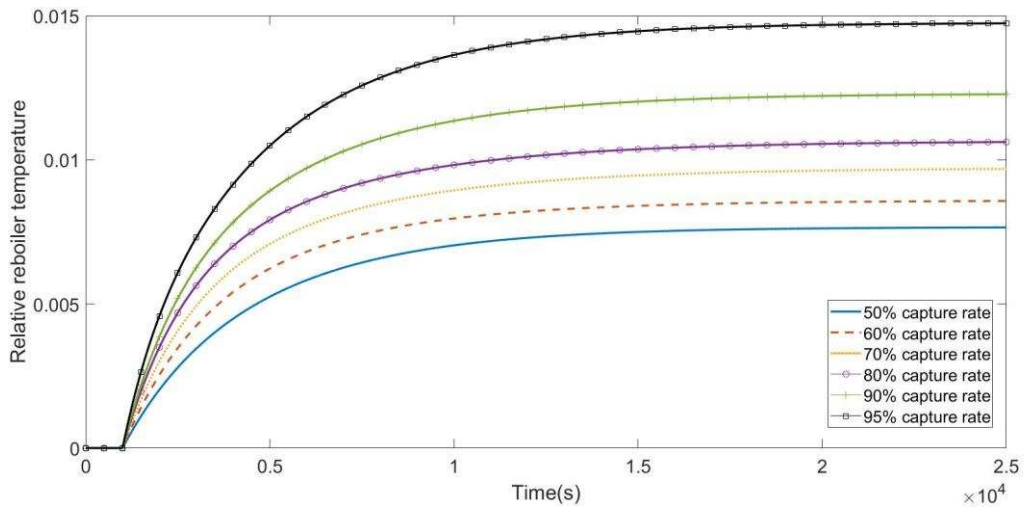


Fig. 8. Relative reboiler temperature with the step change in steam flowrate

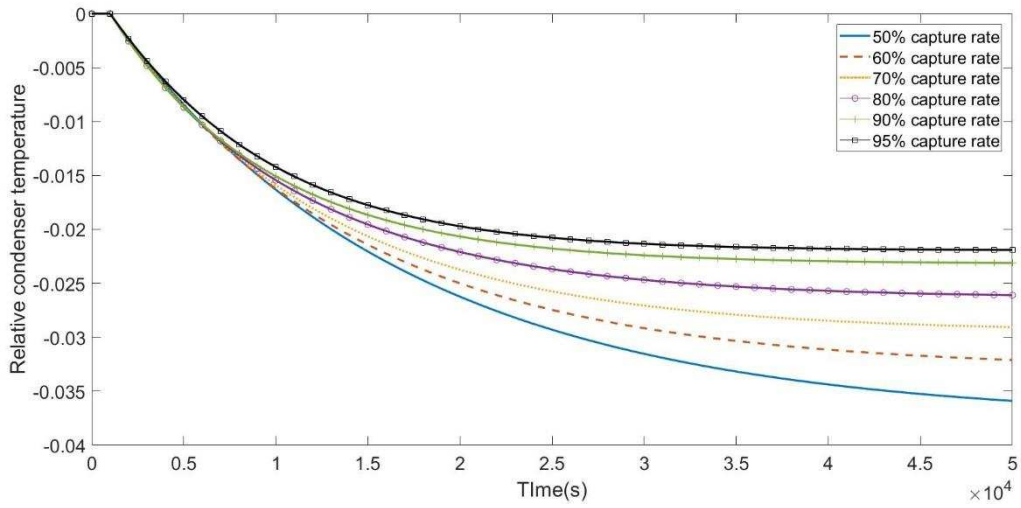


Fig. 9. Relative condenser temperature with the step change in cooling water flowrate to condenser

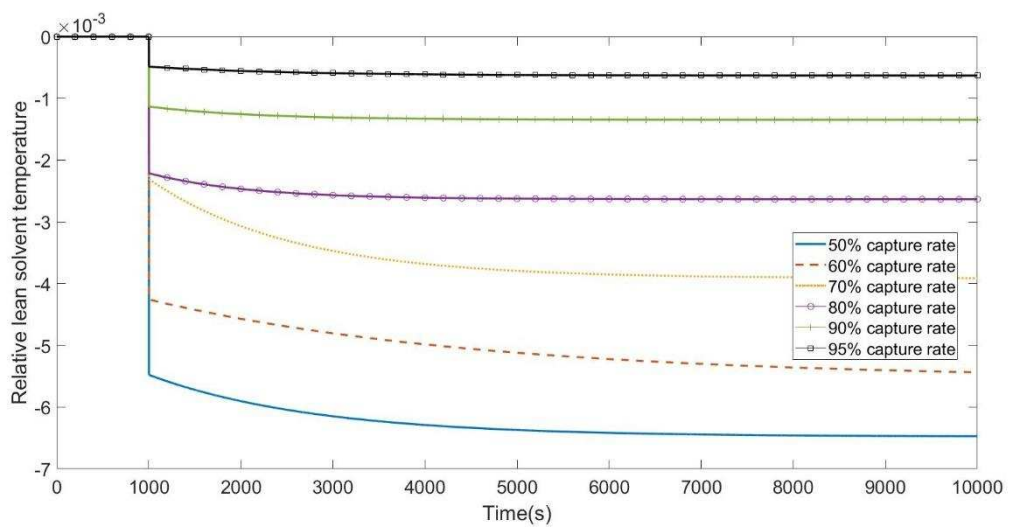


Fig. 10. Relative lean solvent temperature with the step change in cooling water flowrate to cooler

250  
251  
252

253  
254  
255

256  
257

259 A sensitivity analysis is carried out using the input variable perturbation method. This analysis provides a quantitative evaluation  
 260 of outputs relating to possible changes in input variables. The relative input data along with their sensitivity index (relative outputs)  
 261 are portrayed in Table 3. Sensitivity analysis can provide information in the process dynamics and are able to calculate process  
 262 gains. According to the results, there is an inverse correlation between lean solvent flowrate ( $u_1$ ) and capture rate ( $y_1$ ). A similar  
 263 correlation can be found between condenser cooling water flowrate ( $u_3$ ) and condenser temperature ( $y_3$ ) as well as cooler cooling  
 264 water flowrate ( $u_4$ ) and lean solvent temperature ( $y_4$ ).  $u_1$  has a strong effect to its corresponding output  $y_1$ , while  $u_2, u_3, u_4$  are much  
 265 less influential towards their outputs ( $y_2, y_3, y_4$ ). This indicates that the controller gain designed for  $u_1$ - $y_1$  model should be smaller  
 266 than those in  $u_2$ - $y_2, u_3$ - $y_3$  and  $u_4$ - $y_4$  models. Furthermore, the sensitivity index changes with the variation of capture rates. Indexes  
 267 of models in  $u_1$ - $y_1, u_2$ - $y_2$  and  $u_3$ - $y_3$  loops has a narrow change at different capture rates, while the index in  $u_4$ - $y_4$  loop varies rapidly.  
 268 This supports the nonlinearity analysis obtained in Section 5.1.

269 ■ Table 3. Sensitivity analysis of 4 SISO models

Inputs( $u_i$ )	Step changes	Sensitivity Index (Output $\Delta y_i$ )						
		$\Delta y_i(50\%)$	$\Delta y_i(60\%)$	$\Delta y_i(70\%)$	$\Delta y_i(80\%)$	$\Delta y_i(90\%)$	$\Delta y_i(95\%)$	
$\Delta u_1$	10%	-0.1729	-0.1966	-0.2178	-0.2355	-0.2447	-0.2360	$\Delta y_1$
$\Delta u_2$	10%	0.0077	0.0086	0.0097	0.0106	0.0123	0.0147	$\Delta y_2$
$\Delta u_3$	10%	-0.0359	-0.0321	-0.0291	-0.0261	-0.0231	-0.0219	$\Delta y_3$
$\Delta u_4$	10%	-0.0065	-0.0054	-0.0039	-0.0026	-0.0013	-0.00063	$\Delta y_4$

## 270 5. Nonlinearity analysis

271 With variation in operating conditions, dynamic characteristics of solvent-based PCC plant may change and exhibit an inherent  
 272 nonlinearity. Using the local models developed in Section 3.3, this section provides a nonlinearity analysis based on gap metric to  
 273 quantify the nonlinearity degree of PCC process (as modelled in gCCS). Compared with [10], this paper put more key variables  
 274 (As listed in Table 1) in consideration to investigate their nonlinear characteristics in a quantitative manner. Nonlinearity  
 275 measurement is also carried out in SISO model to reveal the relationship between input and output variables at varying capture  
 276 rates. These discussions set this section apart from the similar work in [10].

277 The notion of gap to measure distance between nonlinear system was explained in Zams and El-Sakkary [28]. In the same paper,  
 278 gap metric was firstly introduced to capture the uncertainty in feedback system. Later it was found that gap metric is more suitable  
 279 to measure the distance between two linear systems than using a norm-based metric calculation [29]. This section is to use a  
 280 differential gap metric defined in [30] to measure the distance between two linear models. The method used in [30] is more  
 281 applicable and feasible in real process. The gap metric is defined by Equation (2):

$$282 \delta_d(N_1, N_2) = \max \left\{ \bar{\delta}_d(N_1, N_2), \bar{\delta}_d(N_2, N_1) \right\} \quad (2)$$

283 where:

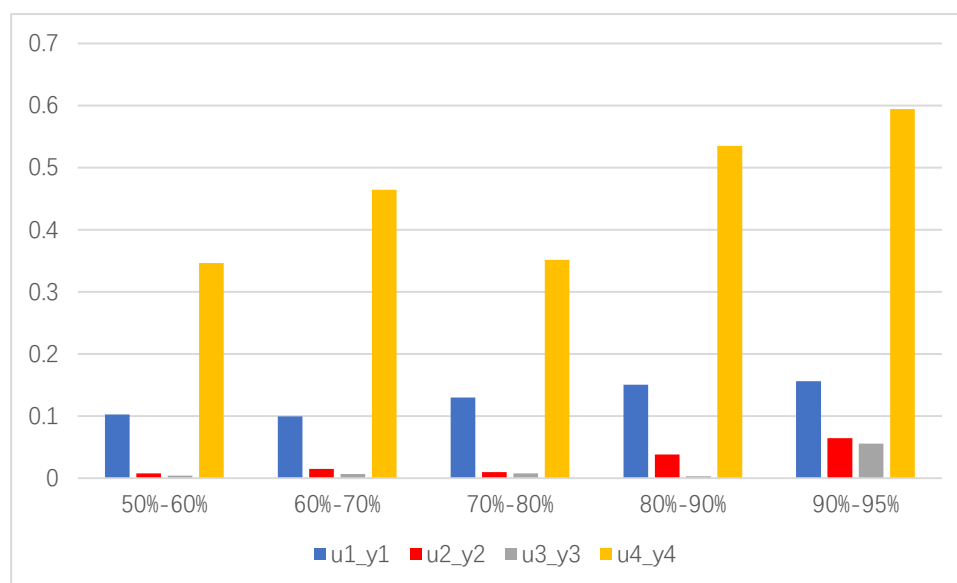
$$284 \bar{\delta}_d(N_1, N_2) = \sup_{r_1} \inf_{r_2} \delta_d(L_{r_1} N_1, L_{r_2} N_2)$$

$$285 \delta_d(L_{r_1} N_1, L_{r_2} N_2) = \left\| \Pi_{G(L_{r_1} N_1)} - \Pi_{G(L_{r_2} N_2)} \right\|$$

286  $L_{r_i} N_i$  represents the linear approximation model of  $N_i$  at the point of  $r_i$  and  $L$  denotes linearization.  $\Pi$  represents the  
 287 rectangular projection and  $G$  is the subspace of the product Hilbert space. SISO transfer functions will be used in Section 5.1 and  
 288 MIMO transfer function matrix will be used in Section 5.2.

292 Due to space limits, only the nonlinear evaluation of models in 4 major control loops (as listed in Table 1) is presented in this  
 293 section. From the results displayed in Fig. 11, it is clear that nonlinearity degrees for lean solvent flowrate ( $u_1$ ) - capture rate ( $y_1$ ),  
 294 steam flowrate ( $u_2$ ) – reboiler temperature ( $y_2$ ), condenser cooling water flowrate ( $u_3$ ) – condenser temperature ( $y_3$ ) models are very  
 295 small, while the degree for cooler cooling water flowrate ( $u_4$ ) – lean solvent flowrate ( $y_4$ ) model is very large compared with the  
 296 other 3 models.

297 This demonstrates that the nonlinearities of models in  $u_1$ - $y_1$ ,  $u_2$ - $y_2$ ,  $u_3$ - $y_3$  control loops are weak and evenly distributed within the  
 298 50%-95% capture rate operating range. The models in these 3 loops are close to the models in their adjacent working condition.  
 299 However, the disparity in model output results (with same inputs) between low and high working conditions (e.g. 50% capture rate  
 300 and 90% capture rate) can be very large. The  $u_4$ - $y_4$  model shows a strong nonlinear behavior with varying working conditions. The  
 301 results obtained in this section are in consistent with the open-loop step response tests in Figs. 7-10.  
 302



303 Fig 11. Nonlinearity degree of SISO system  
 304

## 305 5.2. Nonlinearity analysis of MIMO system

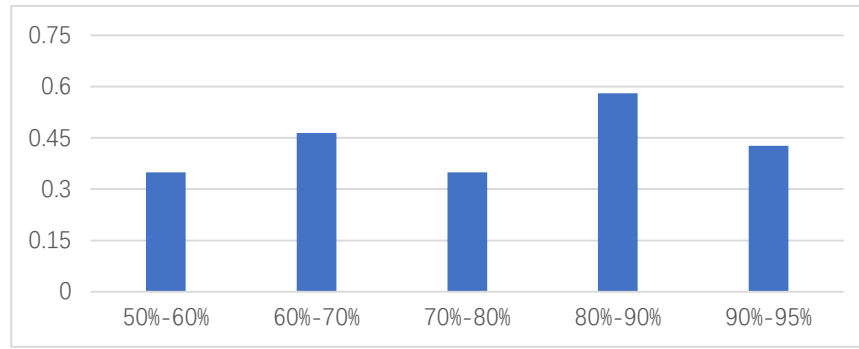
306 In this section, a nonlinear gap measurement of MIMO system is attempted to discover the nonlinear characteristics of the overall  
 307 system. The 4-input-4-output system is expressed in Equation (3), where  $g_{ij}$  denotes the transfer function model in the loop from  
 308  $u_j$  to  $y_i$ . Details of transfer function  $g_{ij}$  can be found in the Appendix.  
 309

$$310 \text{ System 1: } \begin{bmatrix} y_1 \\ y_2 \\ y_3 \\ y_4 \end{bmatrix} = \begin{bmatrix} g_{11} & g_{12} & g_{13} & g_{14} \\ g_{21} & g_{22} & g_{23} & g_{24} \\ g_{31} & g_{32} & g_{33} & g_{34} \\ g_{41} & g_{42} & g_{43} & g_{44} \end{bmatrix} \begin{bmatrix} u_1 \\ u_2 \\ u_3 \\ u_4 \end{bmatrix} \quad (3)$$

311 The results of nonlinear evaluations of System 1 are portrayed in Fig. 12. From this figure, the nonlinearity degree is very large  
 312 in any two adjacent load conditions. This may be due to the strong nonlinear properties in the model of  $u_4$ - $y_4$  loop. This reveals that  
 313 the controller tuned for a certain capture rate (e.g. 90% capture rate) can only function in the vicinity of the mentioned capture rate.  
 314 The control performance may deteriorate if this tuned controller is used for much lower capture rates scenario.

315 According to the open-loop step response test and nonlinearity analysis, PCC plant exhibits strong nonlinearity at varying capture  
 316 rates. This indicates that the linear local models are not sufficiently enough to simulate the nonlinear dynamic characteristics. Given  
 317 this context, it is necessary to develop a piece-wise model by a combination of linear local model in order to predict the nonlinear  
 318 features of PCC process. Using more local models to develop such a piece-wise model will give more accurate prediction results

319 [19]. However, this will also increase the complexity in model implementation and calculation. Considering its evenly distributed  
 320 nonlinearity of MIMO system, the local models in 50%, 60%, 70%, 80%, 90% and 95% capture rate are therefore selected to form  
 321 the piece-wise model.



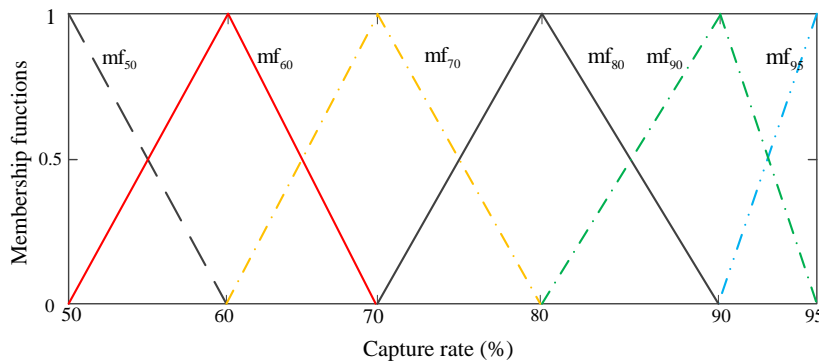
322  
323 Fig. 12. Nonlinearity degree of MIMO system

## 324 6. Piece-wise model and model comparison

### 325 6.1. Fuzzy-based piece-wise model

326 According to the open-loop step response test and nonlinearity analysis of PCC process in the previous sections, the model  
 327 dynamic characteristics differ significantly with varying capture rates. To this end, the identified models in Section 3.3 are selected  
 328 to develop the piece-wise model in order to predict the nonlinear characteristics of PCC process. The unification of the local linear  
 329 models is based on the concept of fuzzy sets theory [31]. This makes the fuzzy model simpler in application.

330 In this section, the Takagi and Sugeno (TS) fuzzy modelling method [32] is adopted to combine the local linear models. The  
 331 first step is to determine the fuzzy variables and their working range. Capture rate is used as scheduling variable. Owing to the  
 332 targets to carry out in this study, capture rate is studied from 50% to 95%. In Fig. 13, a six-rule fuzzy triangular membership  
 333 function of lean solvent flowrate – capture rate model is given as an example.



334  
335 Fig. 13. Membership functions of lean solvent flowrate – capture rate model

336  
337 With the membership function, the output of piece-wise model can be derived from Equation (4):

$$338 \quad y_{\text{Model}} = h_1(mf_{50}) \times y_{50} + h_2(mf_{60}) \times y_{60} + h_3(mf_{70}) \times y_{70} + h_4(mf_{80}) \times y_{80} \\ + h_5(mf_{90}) \times y_{90} + h_6(mf_{95}) \times y_{95} \quad (4)$$

339 where  $h_i(mf_j)$  denotes the triangular weighting functions and  $y_j$  denotes the output of local transfer function in the  $j$  th capture rate.  
 340  $h_i(mf_j)$  can be obtained from the triangular functions in Figure. 13 and  $\sum h_i(mf_j)$  equals to 1.

341 Simulink was used to develop the fuzzy-based piece-wise model. The details of the model structures are described in Fig. 14.  
 342 The models of other control loops, e.g. steam flowrate to reboiler temperature model, condenser cooling water flowrate to  
 343 condenser temperature model and cooler cooling water flowrate to lean solvent temperature model, can be obtained in the same  
 344 manner.

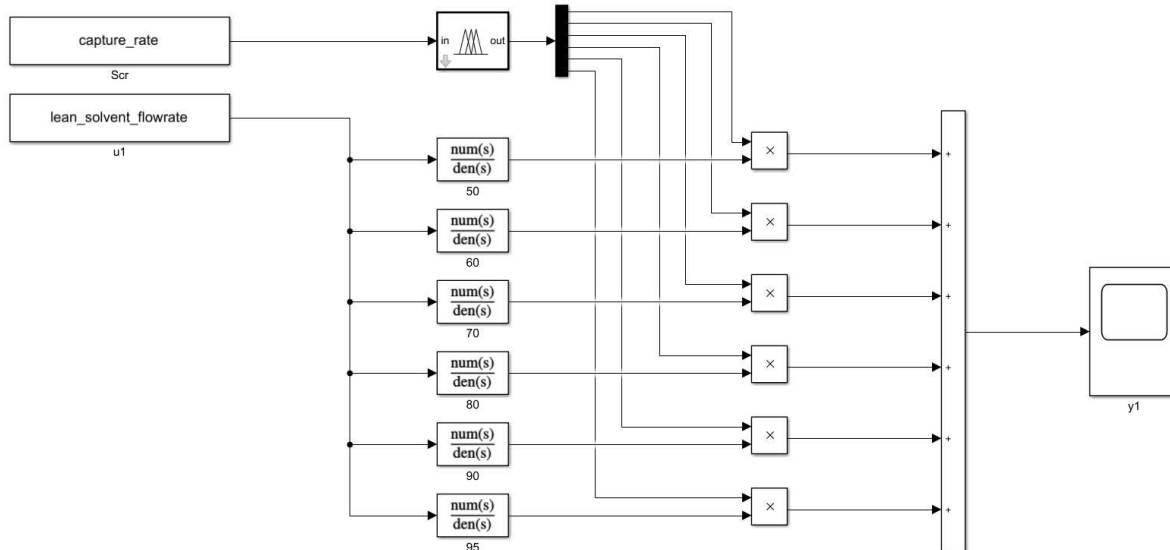


Fig. 14. The piece-wise lean solvent flowrate – capture rate model in Simulink workspace

## 6.2. Model comparison

In this section, the proposed piece-wise models are compared with local linear models and simulation data in the wide-range variation of capture rates. The significance of this comparison is to demonstrate the accuracy of developed piece-wise model in predicting performance of solvent-based PCC plant at different operating conditions.

Due to space limits, the piece-wise models in main 4 control loops (in Table 1) are presented as examples. For simplicity, 4 scenarios are presented in this section, which include:

- The piece-wise lean solvent flowrate to capture rate model is compared with local model (developed at 90% capture rate) and simulation data (collected around 92.5% capture rate).
- The piece-wise steam flowrate to reboiler temperature model is compared with local model (developed at 70% capture rate) and simulation data (collected around 75% capture rate).
- The piece-wise condenser cooling water flowrate to condenser temperature model is compared with local model (developed at 60% capture rate) and simulation data (collected around 65% capture rate).
- The piece-wise cooler cooling water flowrate to lean solvent temperature model is compared with local model (developed at 50% capture rate) and simulation data (collected around 55% capture rate).

Local models were identified for a given set of capture rates (in Section 3.3) and then combined to obtain the piece-wise models (in Section 6.1). The piece-wise models are compared with simulation data from other capture rates different from the given set. Therefore, the validity of the piece-wise model in simulating the performance of PCC plant at varying operating conditions is proven.

The comparison results are given in Figs. 15-18. As shown in Fig. 15 and Fig. 18, it is clear that the piece-wise models are in good agreement with simulation data and are more accurate compared to local models. The results indicate a high level of divergence between piecewise and the local models. However, the disparity between piecewise and the local model in Fig. 15 is much narrow in comparison to the result in Fig. 18. This reveals a much stronger nonlinearity in cooler. A local linear model is not enough to simulate the nonlinear features of cooler unit.

Nevertheless, from Fig. 16-17, it is obvious that the output results of the local models are close to those of the piece-wise models. This is due to the weak nonlinear effects of reboiler and condenser on the process of the PCC plant. The weakness of their nonlinear effects can be demonstrated by their large time constant, which slows down the variation of dynamic feature with the changing of input variables. This means that the number of local linear models for piece-wise combination can be reduced.

In conclusion, the proposed fuzzy-based piece-wise model can satisfactorily simulate the dynamic characteristics of PCC plant over a wide range of operating conditions. The comparisons in these figures reveal strong nonlinearity in cooler, while much weaker nonlinearities in reboiler and condenser. These results are in consistent with the conclusion displayed in Fig. 11.

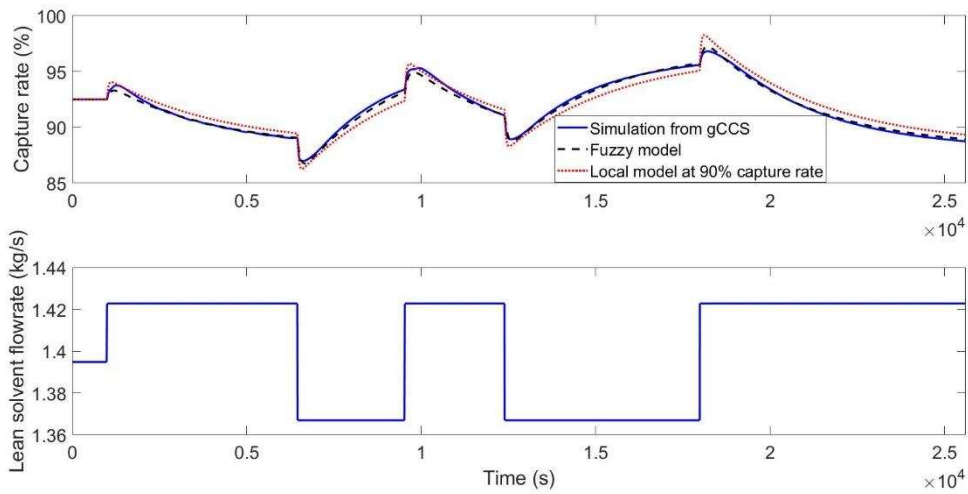


Fig. 15. Comparison of piece-wise lean solvent flowrate – capture rate model around 92.5% capture rate

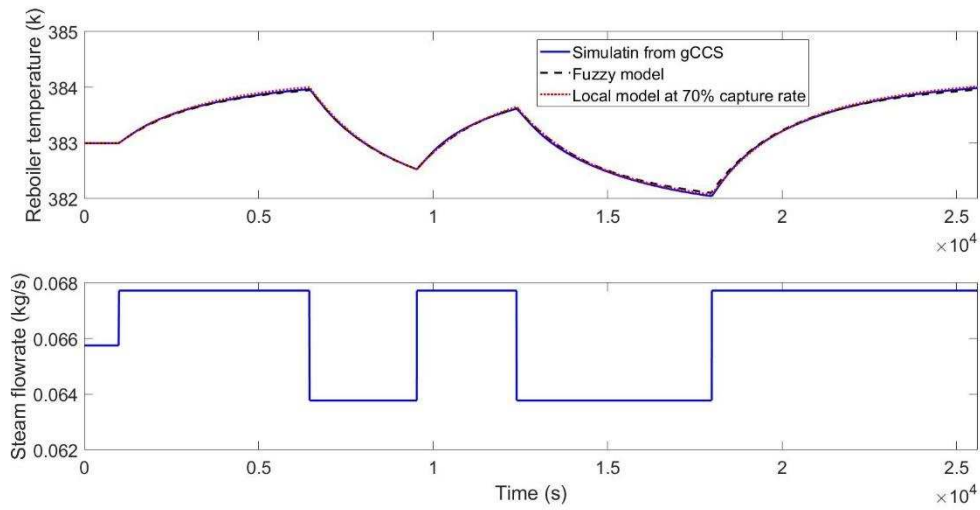


Fig. 16. Comparison of piece-wise steam flowrate – reboiler temperature model around 75% capture rate

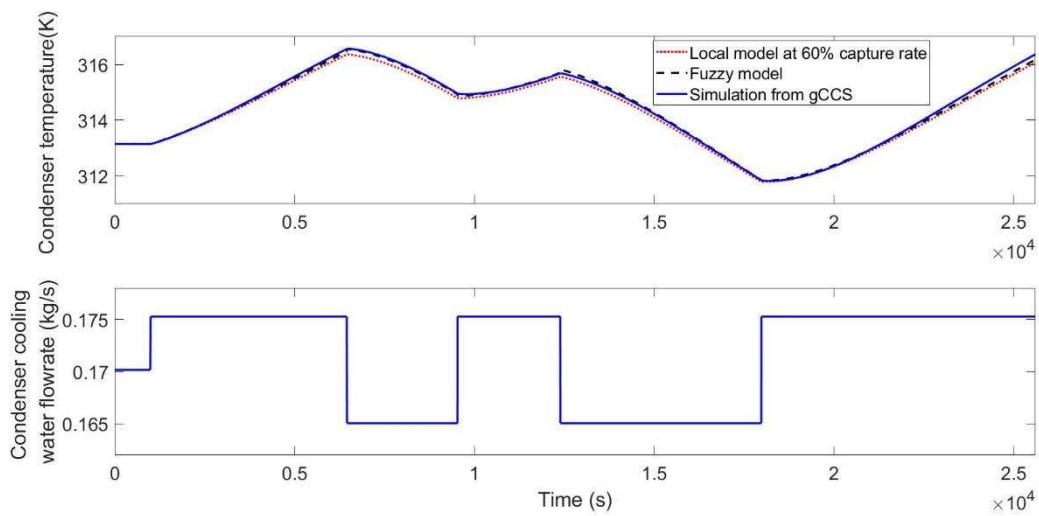


Fig. 17. Comparison of piece-wise condenser cooling water flowrate – condenser temperature model around 65% capture rate

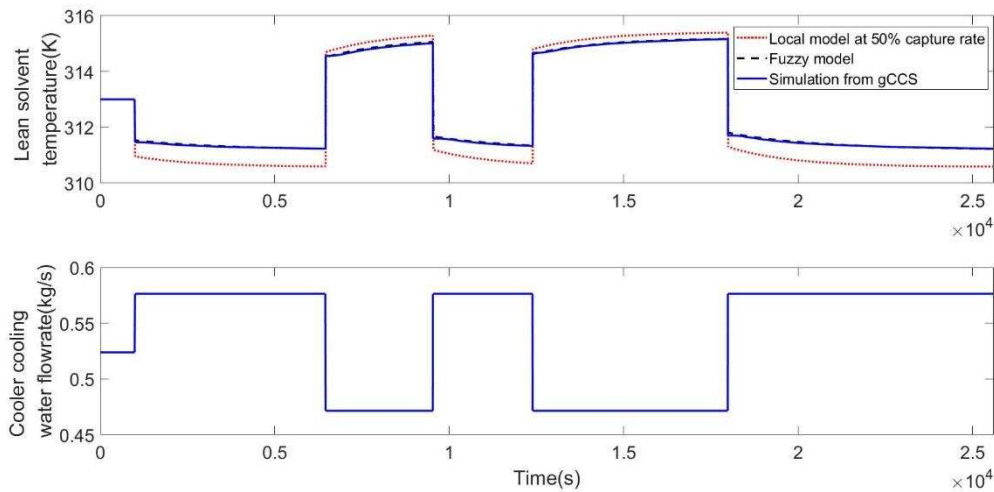


Fig. 18. Comparison of piece-wise cooler cooling water flowrate – lean solvent temperature model around 55% capture rate

## 7. Conclusion

On the basis of system identification and nonlinearity analysis, this paper developed a piece-wise model to simulate the nonlinear dynamic characteristics of the solvent-based PCC process. The piece-wise model shows satisfactory agreement with comparison data and it is more accurate compared with local models. Using simulation data from gCCS software, SISO local transfer function models were firstly identified at every capture rate scenario. Open-loop step response tests were then introduced to show the dynamic features of PCC plant under changing operating conditions. Lean solvent flowrate was found to be very influential on capture rate. The nonlinearity analysis was then carried out using differential gap metric. It was found that the nonlinearity degrees in lean solvent flowrate - capture rate model, steam flowrate – reboiler temperature model and condenser cooling water – condenser temperature model are very small for any two adjacent operating conditions. However, the cooler cooling water flowrate to lean solvent temperature model produces results which exhibit high divergence. Nonlinearity degrees of MIMO PCC system are proven to be equally high in any two operating conditions. The results of this study will provide an enhanced knowledge of transient performance of PCC process and provide guidance for the flexible controller design.

## Acknowledgements

The authors would like to acknowledge the National Natural Science Foundation of China (NSFC) under Grant 51506029, the Natural Science Foundation of Jiangsu Province, China under Grant BK20150631, China Postdoctoral Science Foundation, EU FP7 International Staff Research Exchange Scheme on power plant and carbon capture (Ref: PIRSES-GA-2013-612230) and China scholarship council (CSC no:201606090176) for funding this work.

## Appendix. Supplementary models

Supplementary models of solvent-based PCC process from 50% capture rate to 95% capture rate in each SISO loop are available.

## References

- [1] Coninck HC, Loos MA, Metz B, Davidson O, Meyer LA. IPCC special report on carbon dioxide capture and storage. Intergovernmental Panel on Climate Change 2005.
- [2] DTI UK. Meeting the energy challenge: A white paper on energy. Department for Trade and Industry, Cm7124, 2007.
- [3] Wang M, Lawal A, Stephenson P, Sidders J, Ramshaw C. Post-combustion CO<sub>2</sub> capture with chemical absorption: a state-of-the-art review. Chemical Engineering Research and Design 2011; 89: 1609-1624.
- [4] Abu-Zahra MR, Schneiders LH, Niederer JP, Feron PH, Versteeg GF. CO<sub>2</sub> capture from power plants: Part II. A parametric



- 415 study of the economic performance based on mono-ethanolamine. *International Journal of Greenhouse Gas Control* 2007;  
416 1(2): 135-142.
- 417 [5] Lawal A, Wang M, Stephenson P, Koumpouras G, Yeung H. Dynamic modelling and analysis of post-combustion CO<sub>2</sub>  
418 chemical absorption process for coal-fired power plants. *Fuel* 2010; 89: 2791-2801.
- 419 [6] Lawal A, Wang M, Stephenson P, Yeung H. Dynamic modelling of CO<sub>2</sub> absorption for post combustion capture in coal-fired  
420 power plants. *Fuel* 2009; 88: 2455-2462.
- 421 [7] Lawal A, Wang M, Stephenson P, Obi O. Demonstrating full-scale post-combustion CO<sub>2</sub> capture for coal-fired power plants  
422 through dynamic modelling and simulation. *Fuel* 2012; 101: 115-128.
- 423 [8] Dugas, ER. Pilot plant study of carbon dioxide capture by aqueous mono-ethanolamine. M.S.E. Thesis. University of Texas,  
424 Austin, USA; 2006
- 425 [9] Biliyok C, Lawal A, Wang M, Seibert F. Dynamic modelling, validation and analysis of post-combustion chemical absorption  
426 CO<sub>2</sub> capture plant. *International Journal of Greenhouse Gas Control* 2012; 9: 428-445.
- 427 [10] Wu X, Shen J, Li Y, Wang M, Lawal A. Flexible operation of post-combustion solvent-based carbon capture for coal-fired  
428 power plants using multi-model predictive control: A simulation study. *Fuel* 2018; 220: 931-941.
- 429 [11] Kvamsdal HM, Jakobsen JP, Hoff KA. Dynamic modeling and simulation of a CO<sub>2</sub> absorber column for post-combustion  
430 CO<sub>2</sub> capture. *Chemical Engineering and Processing: Process Intensification* 2009; 48(1): 135-144.
- 431 [12] Ziaii S, Rochelle GT, Edgar TF. Dynamic modeling to minimize energy use for CO<sub>2</sub> capture in power plants by aqueous  
432 mono-ethanolamine. *Industrial & Engineering Chemistry Research* 2009; 48(13): 6105-6111.
- 433 [13] Arce A, Mac Dowell N, Shah N Vega LF. Flexible operation of solvent regeneration systems for CO<sub>2</sub> capture processes using  
434 advanced control techniques: Towards operational cost minimization. *International Journal of Greenhouse Gas Control* 2012;  
435 11: 236-250.
- 436 [14] L. Ljung. *System Identification Toolbox*. For use with Matlab 1995.
- 437 [15] Manaf NA, Cousins A, Feron P, Abbas A. Dynamic modelling, identification and preliminary control analysis of an amine-  
438 based post-combustion CO<sub>2</sub> capture pilot plant. *Journal of Cleaner Production* 2016; 113: 635-653.
- 439 [16] Mac Dowell N, Samsatli NJ, Shah N. Dynamic modelling and analysis of an amine-based post-combustion CO<sub>2</sub> capture  
440 absorption column. *International Journal of Greenhouse Gas Control* 2013; 12: 247-258.
- 441 [17] Li F, Zhang J, Oko E, Wang M. Modelling of a post-combustion CO<sub>2</sub> capture process using neural networks. *Fuel* 2015; 151:  
442 156-163.
- 443 [18] Hamming R. *Numerical methods for scientists and engineers*. Courier Corporation 2012.
- 444 [19] Sontag E. Nonlinear regulation: The piece-wise linear approach. *IEEE Transactions on automatic control* 1981; 26(2): 346-  
445 358.
- 446 [20] Process Systems Enterprise UK. gCCS overview, <http://www.psenterprise.com/products/gccs.html>
- 447 [21] Harun N. Dynamic simulation of MEA absorption process for CO<sub>2</sub> capture from power plant. PhD thesis, University of  
448 Waterloo; 2012.
- 449 [22] Lin YJ, Chang CC, Wong DSH, Jang SS, Ou JJ. Control strategies for flexible operation of power plant with CO<sub>2</sub> capture  
450 plant. *AIChE Journal* 2012; 58: 2697-2704.
- 451 [23] Lin YJ, Pan TH, Wong DSH, Jang SS, Chi YW, Yeh CH. Plantwide control of CO<sub>2</sub> capture by absorption and stripping using  
452 mono-ethanolamine solution. *Industrial & Engineering Chemistry Research* 2010; 50: 1338-1345.
- 453 [24] Nittaya T, Douglas PL, Croiset E, Luis A, Sandoval R. Dynamic modelling and control of MEA absorption processes for CO<sub>2</sub>  
454 capture from power plants. *Fuel* 2014; 116: 672-691.
- 455 [25] Aroonwilas A, Tontiwachwuthikul P, Chakma A. Effects of operating and design parameters on CO<sub>2</sub> absorption in columns  
456 with structured packings. *Separation and Purification Technology* 2001; 24(3): 403-411.
- 457 [26] Yin H, Zhu Z, Ding F. Model order determination using the Hankel matrix of impulse responses. *Applied Mathematics*  
458 *Letters* 2011; 24(5): 797-802.
- 459 [27] Mechleri E, Lawal A, Ramos A, Davison J, Mac Dowell N. Process control strategies for flexible operation of post-  
460 combustion CO<sub>2</sub> capture plants. *International Journal of Greenhouse Gas Control* 2017; 57: 14-25.
- 461 [28] El-Sakkary A. The gap metric: Robustness of stabilization of feedback systems. *IEEE Transactions on Automatic Control*

462 1985; 30(3): 240-247.

463 [29] Georgiou TT, Smith MC. Optimal robustness in the gap metric. IEEE Transactions on Automatic Control 1990; 36(6): 673-  
464 686.

465 [30] Georgiou TT. Differential stability and robust control of nonlinear systems. Signals and Systems 1993; 6(4): 289-306.

466 [31] Zimmermann HJ. Fuzzy set theory and its applications. Springer Science & Business Media, 2011.

467 [32] Takagi T, Sugeno M. Fuzzy identification of systems and its applications to modeling and control. IEEE Transactions on  
468 Systems, Man and Cybernetics 1985; 1: 116-132.

469

470

471